Effect of ambient temperature on the performance of micro gas turbine with cogeneration system in cold region

Firdaus BASRAWI*, Takanobu YAMADA*,δ, Kimio NAKANISHI*
and Soe NAING*

*Kitami Institute of Technology, Department of Mechanical Engineering,
165, Koen-Cho, Kitami City, Hokkaido 090-8507, Japan

δ*Corresponding author*: Tel.: +081-0157-25-7081

E-mail address: yama@mail.kitami-it.ac.jp

Abstract

A small-scale prime mover especially micro gas turbine is a key factor in order to widespread the utilization of biogas. It is well known that a performance of large-scale gas turbine is greatly affected by its inlet air temperature. However, the effect of the inlet air temperature on the performance of small-scale gas turbine (micro gas turbine) is not widely reported. The purpose of the present study is to investigate the effect of the inlet air temperature on the performance of a micro gas turbine (MGT) with cogeneration system (CGS) arrangement. An analysis model of the MGT-CGS was set up on the basis of experimental results obtained in a previous study and a manufacturer standard data, and it was analysed under a various ambient temperature condition in a cold region. The results show that when ambient temperature increased, electrical efficiency η_{ele} of the MGT decreased but exhaust heat recovery η_{ehr} increased. It was also found that when ambient temperature increased, exhaust heat to mass flow rate Q_{exe}/m_e and exhaust heat recovery to mass flow rate Q_{ehr}/m_e increased, with maximum ratios of 259kJ/kg and 200kJ/kg, respectively were found in summer peak. Furthermore, it was also found that the exhaust heat to power ratio Q_{exe}/P_e had a similar

characteristic with exhaust heat recovery to power ratio Q_{ehr}/P_e. Q_{exe}/P_e and Q_{ehr}/P_e increased with the increase of ambient temperature. Moreover, although different values of total energy efficiency, fuel energy saving and CO_2 reduction for every temperature condition were found comparing with a two conventional system that were considered, the MGT-CGS could annually reduce 30000~80000m^3/y of fuel consumption and 35~94t-CO_2/y of CO_2 emissions.

Key words: Micro gas turbine; Cogeneration system; Inlet air temperature; Energy; Efficiency.

1. Introduction

In recent years, the world is facing two energy related threats, rapid depletion of fossil fuel and environmental disruption [1]. One of the possible solutions is by the utilization of biogas with the energy saving technology, cogeneration system (CGS). Biogas has many advantages compared to the fossil fuel, it is a renewable, carbon neutral and since wastes also treated for producing it, it can also help preventing environmental pollution [2] and [3]. The "Biomass Nippon Strategy" was established in Japan in December 2002 in order to use all the unutilized biomass as a product or as energy [4]. While, the measures outlined in the European Union Biomass Action Plan in Europe will lead to an increase in biomass use: by 2010 total biomass consumption will reach approximately 150 Mtoe [5]. Unfortunately, since source of biogas, biomass is scattered in a widerange area with a little amount [2], [6] and [8], the utilization method of it is usually limited to a small-scale biogas plant, or it is transported to a centralised biogas plant. Moreover, since biogas has a low CH_4 content, the application of presently usable prime movers with an output more than a few hundred kilowatts is difficult.

For a prime mover with an output power less than this capacity, a reciprocating engine, a fuel cell and a micro gas turbine (MGT) are available. Among these prime movers, the fuel cell is the most promising technology and gradually becomes available, but it still has a problem with its reliability and still costly

[9], [10] and [11]. While, comparing between the reciprocating engine and the MGT, because of the MGT is a prime mover that offers a multi fuel capability, a high power density, a low maintenance cost and emissions, it attracts attention [12] and [13]. Thus, the utilization of biogas with the micro gas turbine cogeneration system (MGT-CGS) is widespreading and it is proved that MGT-CGS is an efficient system [5], [14], [15], [16], [17], [18] and [19]. In general, the performance of large-scale gas turbine performance is greatly influenced by the inlet air temperature and hence precooling of inlet air is widely proposed [20], [21], [22], [23], [24], [25], [26] and [27]. However, although the application of the MGT is widespreading, there are very limited reports available regarding the effect of the inlet air temperature on the basic performance of the MGT [12], [28], [29], [30], [31] and [32].

In the present study, for a further understanding of the effect of the inlet air temperature on the MGT-CGS performance, an analysis model of the MGT-CGS was set based on experiment results that obtained in a previous study and a manufacturer standard data, and a various operating temperature conditions in the cold region was also considered as an input data. The performance of the analysis model was investigated on the basis of an electrical and heat output efficiency, a mass flow rate, a ratio of heat to mass flow rate and a ratio of exhaust heat to electrical power. Total energy efficiency, fuel energy saving index and CO_2 emissions was also compared with those of conventional systems.

Nomenclature

C	: carbon mass content in the fuel, kg-$_C$/kg-$_{fuel}$
COP	: coefficient of performance, -
$FESI$	: fuel energy saving index, -
h	: enthalpy, kJ/kg
m	: mass flow rate, kg/s
n	: revolution speed of the MGT, rpm
P_e	: electrical power, kW

Q : heat energy, kW

$Q_{S,c}$: standard cooling capacity of the absorption heat exchanger, kW

$Q_{S,h}$: standard heating capacity of the absorption heat exchanger, kW

r , Q_{exe}/P_e : exhaust gas heat to power ratio of the CGS

t : temperature, ^oC

LHV : lower heating value of the fuel, MJ/m^3 or MJ/kg

α : capacity factor of the absorption heat exchanger, -

η : efficiency, -

μ : flow correction factor of the absorption heat exchanger, -

Subscript

a : working fluid in the MGT

an : annual

amb : ambient

$biogas$: biogas

c : cooling cycle

$conv.$: conventional system

co : inlet fluid of cold side in exhaust heat recovery

ci : outlet fluid of cold side in exhaust heat recovery

$co\&ab$: condenser and absorber

CO_2 : carbon dioxide

ehr : exhaust heat recovery

ele : electrical

exe, e : exhaust gas

$fuel$: fuel

g : medium input of the AHE

h : heating cycle

heat : heat

out : outlet fluid of hot side in exhaust heat recovery

t : total energy

tr : total energy recovery

w : water

2. Materials and methods

2.1 Overview of the system and the input data

The schematic diagram of the MGT-CGS analysis model is shown in Fig. 1. The MGT-CGS was mainly composed of the MGT, an exhaust heat exchanger (EHE) and an absorption heat exchanger (AHE). The basic specifications for every part of the CGS are shown in Table 1. The MGT had a 30kW electrical power output and was equipped with a recuperator. Some parameters including turbine outlet temperature, rated revolution speed and electrical power output were set by the previous experimental results and manufacturer standard data.

The all rotating components of the MGT were considered to be mounted on a single shaft supported by air bearings. Atmospheric air enters the MGT systematically passing through a generator, a single stage centrifugal compressor, a recuperator, an annular combustion chamber, a single stage radial turbine and then the recuperator. Pressure ratio, compressor and turbine efficiency, and combustion efficiency were assumed to be equal to 3.4, 0.76 and 0.99, respectively.

The exhaust heat from the MGT was recovered by circulating water coolent in the EHE and the recovered heat was supplied to the AHE. The cold water inlet temperature t_{ci} of the EHE was assumed to be equal to 80˚C. On the basis of experimental data [14], [15] and [16], minimum temperature difference between the cold water inlet and outlet was considered to be equal to 8~10˚C. In order to obtain the optimal heat energy recovery, the temperature exchange efficiency of the EHE was assumed to be equal

to 80% with a capacity ratio range around 0.054~0.063. According to the experimental data [14], [15] and [16], the mass flow rate of the exhaust gas and the cold water were equal to 0.28~0.32 kg/s and 1.616kg/s, respectively.

A LiBr was used as a working fluid in the AHE. Its standard cooling capacity $Q_{s,c}$ and heating capacity $Q_{s,h}$ were 25kW and 35.7kW, respectively. Some portion of the exhaust heat was rejected from the AHE system by a cooling tower and its standard heat rejection capacity was 60.7kW.

The bulk biogas composition that was used in the presented study was typically 50~60% methane and 38~48% carbon dioxide and a small percentage of traces including hidrogen sulfide and water. The bulk biogas ratio was composed of 60% methane and 40% carbon dioxide after the elimination of the traces with lower heating value was around 21.5 MJ/m^3.

2.2 Temperature condition for analysis

Since the MGT-CGS is practically used for an outdoor application, the inlet air temperature was assumed to be equal to the ambient temperature. The ambient temperature in cold region was set by reffering to hourly average temperature changes in an analysis period. The period from May 2004 to April 2005 was used as the analysis period [33]. Since the ambient temperature usually flactuates troughout a year depends on seasons, five ambient temperature conditions were considered. The temperature condition that was set is shown in Table 2. The temperature condition in the analysis period was divided into five temperature conditions: summer, winter, summer peak, winter peak and annual average. The change of a daily average temperature throughout the analysis period is shown in Fig. 2a. As shown in the figure, ambient temperature gradually increased to reach its peak in summer peak and then it decreased again until it reached winter peak.

The last day of summer was 30th September and average ambient temperature on that day was 15°C. As shown in the top right of Fig. 2a, hourly average temperature on the last day of summer was equal to 23ºC in the afternoon which is the most comfortable temperature for humans. Thus, it was assumed that

the period which is colder than this temperature is winter and hotter than this temperature is summer. As shown in Table 2, the duration of winter in the analysis period was longer than summer which was 192 days. The hottest day of the summer peak was in July 25th with a daily average temperature of 28ºC, whereas the coldest day of the winter peak was in January 12th with a daily average temperature of -16ºC.

Hourly average ambient temperature for a 24 hours period for the all temperature conditions is shown in Fig. 2b. As shown in the figure, it is obvious that hourly average temperature for every season varied over daily 24hours. Ambient temperature reached its highest temperature at 12:00 and reached its lowest temperature at 7:00am in all ambient temperature conditions. It was also found that summer peak had a highest temperature of 30ºC and winter peak had a lowest temperature of -15ºC throughout the analysis period.

2.3 Analysis methods

The MGT-CGS was analysed with a Brayton cycle analysis for the MGT, a *NTU-*ε*-*C_R relationship for the EHE and a zero-order model for the AHE. While, a total energy efficiency, a fuel energy saving and a CO_2 emissions of the MGT-CGS plant were compared with a conventional system in order to evaluate its impact. The electrical efficiency η_{ele} of the MGT can be expressed by the ratio of electrical power P_e to fuel energy Q_{fuel} by the following equation:

$$\eta_{ele} = \frac{P_e}{Q_{fuel}} \tag{1}$$

Q_{fuel} can be calculated by its fuel flow rate m_{fuel} and a lower heating value of the biogas LHV_{biogas}. If the lower heating value LHV_{biogas} is assumed to be constant at 21.5MJ/m^3, Q_{fuel} can be expressed by the following equation:

$$Q_{fuel} = m_{fuel}\, LHV_{biogas} \tag{2}$$

Revolution speed n of the MGT is usually changed depends on its inlet air temperature t_{amb}. When ambient temperature increased, it also will be increased for maintaining its rated electrical power output

until a maximum revolution speed is reached. Relation of n with inlet air temperature can be obtained from the experimental data and manufacturer standard data and it can be expressed by the following equations:

$$\begin{aligned} &if\ t_{amb} \le 18.3^{\circ}C, \\ &\quad n = 340 t_{amb} + 89990 \\ &if\ t_{amb} > 18.3^{\circ}C, \\ &\quad n = 96300 \end{aligned} \tag{3}$$

Mass flow rate m_a of working fluid in the MGT was greatly influenced by revolution speed and a density of inlet air. From the experimental data and manufacturer standard data, m_a can be estimated by the following equations:

$$\begin{aligned} &if\ t_{amb} \le 18.3^{\circ}C, \\ &\quad m_a = 0.0005 t_{amb} + 0.3046 \\ &if\ t_{amb} > 18.3^{\circ}C, \\ &\quad m_a = -0.0017 t_{amb} + 0.3444 \end{aligned} \tag{4}$$

If exhaust gas mass flow rate m_{exe} is known, exhaust heat energy Q_{exe} can be calculated from the difference of enthalphy at inlet and outlet of the MGT and hence it can be expressed by the following equation:

$$Q_{exe} = m_{exe}\left[h\left(t_{exe}\right) - h\left(t_{amb}\right)\right] \tag{5}$$

Here, exhaust heat was assumed to be recovered by a shell and tube heat exchanger in which air and water were operated as working fluids. The heat recovered Q_{ehr} can be calculated by the enthalpy changes between inlet and outlet of the air side or the water side. If the mass flow rate of the water m_w can be collected from manufacturer standard data, Q_{ehr} can be obtained by the following equation:

$$Q_{ehr} = m_w\left[h\left(t_{co}\right) - h\left(t_{ci}\right)\right] = m_{exe}\left[h\left(t_{exe}\right) - h\left(t_{out}\right)\right] \tag{6}$$

where t_{ci} and t_{co} represent the inlet and the outlet temperatures of the cold(water) side of the EHE, respectively and t_{exe} and t_{out} represent the inlet and outlet temperatures of the hot(exhaust gas) side of the

EHE, respectively. From the Q_{exe} and Q_{ehr}, efficiencies of the exhaust and recovered heat η_{exe} and η_{ehr} can be expressed as the following equations:

$$\eta_{exe} = \frac{Q_{exe}}{Q_{fuel}} \quad \text{and} \quad \eta_{ehr} = \frac{Q_{ehr}}{Q_{fuel}} \tag{7}$$

The zero-order model [34] was used to analysis the performance of the AHE. Block diagram of the AHE is shown in Fig. 3. The AHE was comprised of two fluids in vapour or liquid phase. The losses in the system and losses by the interactions of the system with the surroundings were neglected in this model. In addition, the overall energy balance for input and output heat energy in the system was assumed to be equal to zero. The input heat energy of the system were heat medium input quantity Q_g and cooling capacity of the AHE Q_c. Thus, sum of the output heat energy from condenser and absorber $Q_{co\&ab}$ can be expressed as the following equation:

$$Q_{co\&ab} = Q_g + Q_c \tag{8}$$

If the AHE is operated in the heating cycle operation, $Q_{co\&ab}$ must be zero and no heat is transfered into the condenser and the absorber. Thus, the heating capacity directly depends on the standard heating capacity $Q_{s,h}$ of the working fluid. If a heating capacity factor α_h and a heat medium flow correction μ can be obtained from the manufacturer standard data, the heating capacity Q_h can be calculated from the standard heating capacity $Q_{s,h}$ by the following equation:

$$Q_h = \alpha_h \times \mu \times Q_{s,h} \tag{9}$$

The same method could be applied for the cooling capacity Q_c of the AHE. If a cooling capacity factor α_c can be found in the manufacturer standard data, Q_c can be expressed by a standard cooling capacity $Q_{s,c}$ by the following equation:

$$Q_c = \alpha_c \times \mu \times Q_{s,c} \tag{10}$$

The performance of the cooling and heating cycles is usually indicated by a *COP* value. Thus, after values from equation (9) and (10) were obtained, the *COP* values were also calculated. The *COP* values of the cooling cycle COP_c and heating cycle COP_h can be expressed by the following equations:

$$COP_C = \frac{Useful\ heat\ moved\ or\ obtained}{Energy\ requirement\ to\ drive\ process} \tag{11}$$

With regards to the relationship between the cooling cycle and the heating cycle of the AHE, *COP* value for the heating cycle COP_h can be expressed by the following equation:

$$COP_h = COP_c + 1 \tag{12}$$

The impact of the MGT-CGS was also investigated by comparing the total energy saving, the fuel energy saving and the reduction of CO_2 emission of the MGT-CGS with the conventional systems. The total energy efficiency was defined to evaluate the effectiveness of energy utilization of the MGT-CGS. The annual total energy efficiency $\eta_{t,an}$ and the annual total energy recovery efficiency $\eta_{tr,an}$ of the MGT-CGS can be expressed as the following equations:

$$\eta_{t,an} = \eta_{exe,an} + \eta_{ele,an} \text{ and } \eta_{tr,an} = \eta_{ehr,an} + \eta_{ele,an} \tag{13}$$

In the present study, the conventional system was equipped with a seperated power plant and boiler. Since the efficiency of the power plant can vary significantly between a typical power plant and a best technology available, a two set of the conventional systems were considered. One was for the typical case with its electrical power generation efficiency $\eta_{ele,conv.}$ and heat generation efficiency $\eta_{heat,conv.}$ were assumed to be equal to 0.37 and 0.85, respectively [29]. An another one was for the best technology available (e. g. combined cycle). $\eta_{ele,conv.}$ and $\eta_{heat,conv.}$ effciencies of the best technology were assumed to be equal to 0.50 and 0.85, respectively. It should be noted that, in order to compare the MGT-CGS with the conventional systems, the electrical power and heat output of the conventional systems were arranged to be equal to the output of the MGT-CGS. Total energy efficiency of the conventional systems $\eta_{t,conv.}$ can be expressed as the following equation:

$$\eta_{t,conv.} = \frac{Q_{conv.} + Pe_{conv.}}{Q_{fuel,conv.}} \tag{14}$$

Moreover, fuel energy saving index *FESI* was also defined to evaluate the impact of the MGT-CGS on a fuel energy saving aspect. If exhaust heat to power ratio of the MGT-CGS is represented by r or Q_{exe}/P_e, the *FESI* of the MGT-CGS can be expressed as the following equation [29]:

$$FESI = 1 - \frac{1+r}{r\eta_{t,an}\left[\frac{1}{r\eta_{ele,conv.}} + \frac{1}{\eta_{heat,conv.}}\right]} \tag{15}$$

Furthermore, the CO_2 emission was also calculated to evaluate the impact of the MGT-CGS on a environmental benefit. If a complete combustion with an excess air in a combustion chamber which is also in a good operating condition is assumed, mass of emitted CO_2 can generally be expressed as the following equation [35]:

$$m_{CO_2} = \frac{44C \times Q_{exe}}{12\eta_{exe} \times LHV_{biogas}} \tag{16}$$

where a typical value of C was assumed to be equal to 75% of the fuel compound, and fuel consumption was obtained from ratio of exhaust heat to its efficiency.

3. Results and discussions

3.1 Validation of the analysis model

The analysis model of the MGT-CGS was validated by the comparison of the analytical results with the experimental results that was obtained in the previous studies [14] and [15]. In the previous studies, the adaptability of the MGT-CGS was investigated initially under cold temperature condition by using kerosene as a fuel, and then by using biogas. A part of the results that show a notable relation of ambient temperature with the important parameters of the MGT-CGS are shown in Fig. 4. Both solid and doted lines represent the analytical results and the symbols represent the experimental result. The analytical results of the model with three different turbine and compression efficiencies of 0.76, 0.86 and 0.96 are also shown in Fig. 4. It should be noted that these results were obtained when all design conditions including the turbine inlet temperature, the pressure ratio and revolution speed of the analysis model were

same except for the turbine and compressor efficiency. Exhaust temperature and the mass flow rate are shown in Fig. 4a, exhaust heat and electrical power are shown in Fig. 4b, Enthalpy at exhaust and compressor inlet stage are shown in Fig. 4c, and exhaust heat recovery, heat losses and heat to power ratio are shown in Fig. 4d.

As shown in Fig. 4a, when ambient temperature increased, exhaust temperature also increased. It was also found that the mass flow rate increased slightly until ambient temperature reached 18°C, and it decreased over that. Since air density decreased when ambient temperature increased, mass flow rate and turbine work also decreased, while compressor work increased. Thus, the MGT was designed to increase its revolution speed when the temperature increased in order to maintain its rated electrical power output, until the maximum revolution speed is reached. Since maximum revolution speed reached when ambient temperature increased until 18°C, and mass flow rate decreased over this temperature.

As shown in Fig. 4b, when ambient temperature increased from -15~18°C, exhaust heat increased, while electrical power output remained to be constant at 29kW. When ambient temperature increased higher than 18°C, exhaust heat energy gradually decreased, while electrical power output decreased to 20kW. Since revolution speed of the MGT was controlled to maintain its rated electrical power output, when ambient temperature increased from -15~18°C, electrical power output remained to be constant. While, exhaust heat gradually increased because of exhaust temperature and mass flow rate also gradually increased. Since mass flow rate decreased when ambient temperature increased higher than 18°C, both electrical power and exhaust heat decreased.

As shown in Fig. 4c, when ambient temperature increased, enthalpies at compressor inlet and exhaust stage increased. This is because gas temperature in the both stages also increased when temperature increased. As shown in Fig. 4d, when ambient temperature increased until 18°C, exhaust heat recovery also increased, and it only gradually increased over that temperature. Although exhaust heat decreased when ambient temperature increased more than 18°C, exhaust heat recovery still increased due to the

reduction of heat losses to the environment as shown in the same figure. It was also found that when ambient temperature increased, exhaust heat to power ratio gradually increased.

The model analysed with a turbine and a compressor of a different efficiencies. As also shown in Fig. 4, it was obvious that more electrical power output but less heat can be obtained when the turbine and the compressor of higher efficiencies were used. Thus, a MGT with a lower heat to power ratio can be obtained if turbine and compressor of higher efficiency are used in the MGT.

A quantitive error of the experimental results to the calculation results was also investigated. Each average of an absolute value of errors to the calculated value and its percentage for the exhaust temperature were 1.5°C and 0.5%, 0.002kg/s and 0.5% for mass flow rate, 0.23kW and 0.3% for exhaust heat energy, 1.4kW and 5.1% for electrical power output, 1.6kJ/kg and 0.3% for enthalpy value in the exhaust stage, 0.99kJ/kg and 0.3% for enthalpy value in the compressor inlet stage, 0.15kW and 0.3% for exhaust heat recovery, 0.38kW and 1.9% for heat losses, and 0.14 and 5.1% for heat to power ratio, respectively. Therefore, although some error was confirmed, Fig. 4 shows that results from the analysis model were approximately agreed with the experiment results which ensure that analysis model was valid.

A very similar trend in electrical power output with results that was obtained in the presented study has also been reported [12] and [28]. The Capstone Turbine Corporation studied with a 30kW capacity MGT and reported that when ambient temperature increased electrical power remained constant with a 30kW output until 18°C, and electrical power output decreased over that temperature [12]. An another report also shows similar result, when ambient temperature increased electrical power remained constant with a 28kW output until 15°C, and electrical power output decreased over that temperature [28]. On the other hand, another research group [32] reported that, when temperature increased electrical power remained constant with a 30kW output until -14°C, and electrical power output decreased over that temperature. This lower output power may be due to recuperator was not used in the MGT. Although only

relation of electrical power and temperature is available on those reports, it proved that the analysis model results were agreed with other report.

3.2 Performance of the CGS

The variation of electrical efficiency with respect to the temperature conditions is shown in Fig. 5. As shown in Fig. 5, highest electrical efficiency was found during winter peak, whereas the lowest electrical efficiency was found during summer peak. It was also found that minimum electrical efficiency was obtained around 12:00~13:00pm for all ambient temperature conditions. It decreased up to 23.6% at 12:00 during summer peak.

The variations of mass flow rate and exhaust temperature for all temperature conditions are shown in Fig. 6a. As shown in Fig. 6a, since revolution speed of the MGT is controlled to maintain its rated electrical power output, it was found that when the temperature condition changed from winter peak to summer peak, generally mass flow rate gradually increased but different curves were found in the summer and the summer peak. Mass flow rate of the MGT was found decreased at 7:00~18:00 in summer and at 5:00~24:00 in summer peak. Mass flow rate started to decrease because its revolution speed reached to the maximum. Minimum mass flow rate was equal to 0.294kg/s at 12:00 in summer peak, and maximum mass flow rate was equal to 0.314kg/s at 9:00 in summer period. The effect of the variation of mass flow rate on the exhaust heat is shown in the same figure. It was found that when the temperature condition changed from winter peak to summer peak, exhaust heat increased except for the summer peak. This is because of mass flow rate was significantly decreased in summer peak. The highest exhaust heat, 80kW was obtained at 10:00 in summer, whereas the lowest exhaust heat was obtained at 7:00 in winter.

The effect of the ambient temperature on the efficiency of exhaust heat η_{exe}, exhaust heat recovery η_{ehr} and electrical η_{ele} of the CGS is shown in Fig. 6b. It should be noted that the error bars indicate a borders between a different temperature conditions. As shown in Fig. 6b, when ambient temperature increased, efficiency of exhaust heat and exhaust heat recovery increased but efficiency of electrical

power decreased. From the analysis results, it was found that when ambient temperature was at 10°C, η_{ele}, η_{ehr} and η_{exe} were equal to 0.26, 0.46 and 0.67, respectively. In practical, heat demand of a facility where the MGT is used usually decreases in summer, while electrical demand increases because demand of air conditioning. However, as shown in the result, the heat energy efficiencies of the MGT-CGS in summer are higher and electrical power is lower. Thus, inlet precooling is particularly important in summer to match the electrical and heat output of the MGT-CGS for the electrical and heat demand of a facility.

The other performances of the CGS such as ratio of heat energy to exhaust mass flow rate, and ratio of heat energy to electrical power for all seasons are presented in Fig. 7. The MGT-CGS is practically used in a widerange application including direct use of exhaust heat for snow melting, use of recovered heat for heating purpose only, or use of recovered heat with an AHE for cooling and heating purposes. Thus, these applications were considered and a heat energy performance of the MGT-CGS for every stage was investigated. These results are shown in Fig. 7a, Fig. 7b, Fig. 7c and Fig. 7d. In addition, since heat to power ratio is also important index to compare one CGS to another CGS, heat to power ratio for every stage is also shown in Fig. 7e and Fig. 7f.

The variations of ratio of exhaust heat to mass flow rate Q_{exe}/m_e and ratio of exhaust recovery heat to mass flow rate Q_{ehr}/m_e are shown in Fig. 7a and Fig. 7b. As shown in the figures, when ambient temperature increased, Q_{exe}/m_e and Q_{ehr}/m_e increased. However, different curve was found in summer peak. Q_{exe}/m_e in Fig. 7a remained constant in summer peak because of the both exhaust heat and mass flow rate as shown in previous Fig. 6a decreased at 5:00~24:00. The Q_{exe}/m_e and Q_{ehr}/m_e ratios reached its maximum values, 259kJ/kg and 200kJ/kg, respectively in the summer peak. Whereas, the Q_{exe}/m_e and Q_{ehr}/m_e ratios reached their minimum values, 234kJ/kg and 136kJ/kg, respectively in winter peak.

The performance of the AHE is shown in Fig. 7c and Fig. 7d. It should be noted that the performance of heating cycle was investigated for annual average, winter and winter peak, and the performance of cooling cycle was investigated in summer and summer peak. The maximum value of Q_h/m_e was found in annual average, whereas the maximum value of Q_c/m_e was found in summer peak. It was also found that

the heating cycle was more efficient than the cooling cycle. Both COP values also proved this point with the highest COP value of the heating cycle was found in the annual average temperature condition. A different curve was found for cooling cycle in summer peak. In the calculation results, inlet temperature of the heat medium of the AHE (hot water from the HE) was found to be approximately constant in summer peak, *COP* value also remained approximately constant. The highest *COP* value for cooling cycle was equal to 0.8043 in summer peak. While, the lowest *COP* value for heating cycle was equal to 1.797 in winter peak.

As shown in Fig. 7e, Q_{exe}/P_e increased when temperature condition changed from winter peak to summer peak, and it was also found that Q_{exe}/P_e was higher at 12:00 for all temperature conditions. The highest Q_{exe}/P_e, 2.94 was found at 12:00 in the summer peak, whereas the lowest Q_{exe}/P_e, 2.40 was found at 07:00 in the winter peak. As shown in Fig. 7f, Q_{ehr}/P_e had almost same characteristics with Q_{exe}/P_e, Q_{ehr}/P_e was also found higher at 12:00, and it also increased when temperature condition changed from winter peak to summer peak. The highest Q_{ehr}/P_e, 2.27 was found at 12:00 in the summer peak, whereas the lowest Q_{ehr}/P_e, 1.39 was found at 07:00 in the winter peak. From the above-stated results, if relation of the heat and electrical output of the MGT-CGS and a heat and electrical output of a facility is clarified, one could decide whether inlet air precooling is required or not. Also one could decide to not use directly the AHE for cooling a room but use it for cooling inlet air of the MGT as a method to increase its electrical efficiency in summer.

3.3 Impact of the CGS on energy saving and CO_2 emissions

The CGS was compared to the conventional systems and the impacts of it on the basis of an annual energy efficiency, a fuel energy saving and a CO_2 emissions reduction for all temperature conditions were investigated.

An annual total energy efficiency $\eta_{t,an}$ and an annual total energy recovery efficiency $\eta_{tr,an}$ of the CGS and an annual total energy efficiency $\eta_{t,conv.}$ of the conventional systems for all temperature conditions

used for the analysis are shown in Fig. 8. It should be noted that $\eta_{t,conv.1}$ and $\eta_{t,conv.2}$ represent the conventional system with the best and the typical technology, respectively. As shown in Fig. 8, $\eta_{t,an}$ and $\eta_{tr,an}$ that were found in a range of 0.91~0.93 and 0.64~0.77, respectively were higher than the $\eta_{t,conv2.}$ However, $\eta_{tr,an}$ was found lower than $\eta_{t,conv1}$ in the winter peak. These results conclude that the MGT-CGS is more efficient than the conventional system but its energy recovery efficiency in winter peak maybe lower than the conventional system that equipped with a boiler and a combined cycle power plant.

The fuel energy saving index *FESI* for all temperature conditions and its relation with ambient temperature is shown in Fig. 9. A variation of *FESI* for all temperature conditions are shown in Fig. 9a and Fig. 9c, and a relation of *FESI* with ambient temperature are shown in Fig. 9b and Fig. 9d. It should be noted that results shown in Fig. 9a and Fig 9b are results when the MGT-CGS was compared with the best technology (the conventional system 1), and Fig. 9c and Fig. 9d are results when the MGT-CGS was compared with the typical technology (the conventional system 2).

As shown in Fig. 9, *FESI* of the MGT-CGS when compared with the conventional plant 2 is higher than when it compared with the conventional plant 1. It was also found that only a small difference of *FESI* value was found from winter peak to summer peak with a range of 0.222~0.229 and 0.310~0.325 for Fig. 9a and Fig. 9c, respectively. As shown in Fig. 9b, it was found that *FESI* gradually increased when ambient temperature increased to 13°C, and it gradually decreased over that temperature. The highest value of the *FESI* when compared with the conventional system 2 was found when ambient temperature in a range of 12~14°C. As shown in Fig. 9d, it was found that *FESI* gradually increased when ambient temperature increased to -6°C, and it gradually decreased over this temperature. The highest value of the *FESI* when compared with the typical tecnology of the conventional system was found when ambient temperature in a range of -5~-8°C. The difference between the highest and the lowest *FESI* for each case were 0.015 and 0.007 which means that the operation of the CGS in winter peak could reduced 0.7~1.5% of fuel consumption than those in summer peak.

In order to clarify the impact of the MGT-CGS, reduction in fuel consumption and CO_2 emissions was also investigated. The amount of fuel consumption and CO_2 emissions of the MGT-CGS which compared to the both conventional systems are shown in Fig. 10a and Fig. 10b. It should be noted that the amount of fuel consumption and CO_2 emissions are shown for all temperature conditions that used for the analysis with respect to their number of days. As shown in Fig. 10a, the MGT-CGS could reduce fuel consumption in all temperature conditions. Annually, the CGS could reduce approximately 30000m^3/y and 80000m^3/y of fuel consumption compared to the conventional system1 and conventional system 2, respectively. A similar result could also be found in CO_2 emissions. The CGS could reduce approximately 35t-CO_2/y and 94t-CO_2/y compared to the conventional system1 and conventional system 2, respectively.

4. Conclusions

In this paper, the effect of ambient temperature on the performance of the MGT-CGS was investigated by considering its application under various ambient temperature conditions in cold region and the following results were obtained:

1. It was found that when ambient temperature increased, electrical efficiency decreased but exhausts heat recovery increased.
2. It was also found that when ambient temperature increased, ratio of exhaust heat to mass flow rate Q_{exe}/m_e and ratio of exhaust heat recovery to mass flow rate Q_{ehr}/m_e increased. Maximum ratio of Q_{exe}/m_e, 259kJ/kg and Q_{ehr}/m_e, 200kJ/kg was found in summer peak. It was also found that performance of heating cycle was more efficient than cooling cycle for the AHE.
3. The exhaust heat to power ratio Q_{exe}/P_e had a similar behavior with exhaust heat recovery to power ratio Q_{ehr}/P_e. Q_{exe}/P_e and Q_{ehr}/P_e increased when ambient temperature increased, with highest values, 2.94 and 2.27 were found at 12:00 in summer peak.
4. From the clarification of the MGT-CGS performance under various temperature conditions, the controlling of heat and electrical output of the CGS could be applied. If heat and electrical output of

the MGT-CGS and heat and electrical demand of a facility is known, one could decide whether inlet precooling is required or not.

5. The MGT-CGS was an efficient system on the point of view of total energy efficiency, fuel energy saving, and CO_2 reduction for all temperature conditions. The annual total energy efficiency $\eta_{t,an}$ and the annual total energy recovery efficiency $\eta_{tr,an}$ was found higher than a typical conventional system but $\eta_{tr,an}$ was found lower that a best technology of conventional system in winter. It was also found that the MGT-CGS could annually reduce 30000~80000m^3/y of fuel consumption and 35~94t-CO_2/y of CO_2 emissions.

References

[1] International Energy Agency, World energy outlook (2006), pp. 37.

[2] NTS Co., Ltd., Gaseous fuel fabrication from biomass and its energy utilization (2007), pp. 3-4.

[3] J.B. Holm-Nielsen, T.A. Seadi, P Oleskowicz-Popiel, The future of anaerobic digestion and biogas utilization, *Bioresource Technology* 100 (2009), pp. 5478-5484.

[4] Y. Kuzuhara. Biomass nippon strategy- why "biomass nippon" now?, *Biomass and Bioenergy* 29 (2005), pp. 331-335.

[5] J.C. Bruno, V.O. Lopez, A. Coronas, Integration of absorption cooling systems into micro gas turbine trigeneration systems using biogas: Case study of a sewage treatment plant, *Applied Energy* 86 (2009), pp. 837-847.

[6] C.C. Antonio, P. Mario, M.P. Pacifico, S. Federica, Economics of biomass energy utilization in combustion and gasification plants: effects of logistic variables, *Biomass and Bioenergy* 28 (2005), pp. 35-51.

[7] S. Jagtar, B.S. Panesar, S.K. Sharma, A mathematical model for transporting the biomass to biomass based power plant, *Biomass and Bioenergy* 34 (2010), pp. 483-488.

[8] N.H. Carlo, A.A.S. Roald, P.C.F. Andre, International bioenergy transport costs and energy balance, *Biomass and Bioenergy* 29 (2005), pp. 114-134.

[9] I. Staffell, R. Green, K. Kendall, Cost targets for domestic fuel cell CHP, *Journal of Power Sources* 181 (2008), pp. 339-349.

[10] K. Schoots, G.J. Kramer, B.C.C van der Zwaan, Technology learning for fuel cells: An assessment of past and potential cost reductions, *Energy Policy* 38 (2010), pp. 2887-2897.

[11] P. Zegers, Fuel cell commercialization: The key to a hydrogen economy, *Journal of Power Sources* 154 (2006), pp. 497-502.

[12] Capstone catalogue. Available from:

<http://www.microturbine.com/_docs/datasheets/CR30_331033D_lowres.pdf>.

[13] P.A. Pilavachi, Mini- and micro-gas turbines for combined heat and power, *Applied Thermal Engineering* 22 (2002), pp. 2003-2014.

[14] T. Yamada, T. Yamada, K. Nakanishi, Y. Yamada, Applied research for a sewage treatment center at cold region with MGT co-generation system, *Proceedings of Symposium on Environmental Engineering of JSME* 5-13 (2005), pp. 462-465.

[15] S. Tachibana, T. Yamada, H. Ishitani, Performance of MGT co-generation system in a snowy and cold area. *Proceedings of Annual conference of JSME* 3 (2004), pp. 359-360.

[16] S. Naing, T. Yamada, K. Nakanishi, Renewable Fuel Utilization in a Cogeneration Arrangement with Hydrate Storage Method, *Journal of Power and Energy Systems* 1 (2007), pp.239-250.

[17] Global Case Studies, Capstone Turbine Coorperation official website. Available from: <http://www.capstoneturbine.com/company/global/ >.

[18] L. Dong, H. Liu, S. Riffat, Development of small-scale and micro-scale biomass-fuelled CHP systems – A literature review, *Applied Thermal engineering* 29 (2009), pp. 2119-2126.

[19] K.B. Hur, S.K. Rhim, J.K. Park, Mechanical characteristics evaluation of biogas micro turbine power systems, *Journal of Loss Prevention in the Process Industry* 22 (2009), pp. 1003-1009.

[20] R. Yokoyama, K. Ito, Effect of inlet air cooling by ice storage on unit sizing of a gas turbine cogeneration plant, *Journal of engineering for gas turbines and power* 126 (2004), pp. 351-357.

[21] M.M. Alhazmy, Y.S.H. Najjar, Augmentation of gas turbine performance using air coolers, *Applied Thermal Engineering* 24 (2004), pp. 415-429.

[22] J.P. Bedecarrats, F. Strub, Gas turbine performance increase using an air cooler with a phase change energy storage, *Applied Thermal Engineering* 29 (2009), pp. 1166-1172.

[23] B. Dawoud, Y.H. Zurigat, J. Bortmany, Thermodynamics assessment of power requirements and impact of different gas-turbine inlet air cooling techniques at two different locations in Oman, *Applied Thermal Engineering* 25 (2005), pp. 1579-1598.

[24] O.O. Badran, Gas-turbine performance improvements, *Applied Energy* 64 (1999), pp. 263-273.

[25] F.R.P. Arrieta, E.E.S. Lora, Influence of ambient temperature on combined-cycle power-plant performance, *Applied Energy* 80 (2005), pp. 261-272.

[26] A.M. Bassily, Performance improvements of the intercooled reheat recuperated gas-turbine cycle using absorption inlet-cooling and evaporative after-cooling, *Applied Energy* 77 (2004), pp. 249-272.

[27] H. Caniere, A. Willockx, E. Dick, M.D. Paepe, Raising cycle efficiency by intercooling in air-cooled gas turbines, *Applied Thermal Engineering* 26 (2006), pp. 1780-1787.

[28] S. Tsuzuki, S. Tachibana, T. Yamada, H. Ishitani, M. Sasaki, Experimental study of micro gas turbine at outdoor in cold region, *Proceedings of 31st of Gas Turbine Society of Japan* (2003), pp. 19-23.

[29] S. Naing, T. Yamada, K. Nakanishi, Applied performance research of a cogeneration arrangement with proposed efficiency well-balance method, *Journal of Power and Energy Systems* 1 (2007), pp. 199-210.

[30] Greenhouse Gas Technology Center, Environmental technology verification report: Capstone 60 kW

microturbine CHP system (2003).

[31] Midwest CHP Application Center and Avalon Consulting, Inc., Combined heat & power (CHP) resource guide, Second edition (2005), pp. 11.

[32] U.S. Environmental Protection Agency Combined Heat and Power Partnership, Catalog of CHP Technologies.

[33] Information of weather satistics. Japan Meteorology Agency. Available from: <http://www.jma.go.jp/jma/menu/report.html>.

[34] K.E. Herold, R. Radermacher, Optimum allocation of heat transfer surface in an absorption heat pump, *Proceedings of 25th IECEC* 2 (1990), pp. 217-221.

[35] EDUCOGEN, The European educational tool on cogeneration (2001), pp. 83-84.

Table(s)

Table 1. Basic specifications of the MGT-CGS.

MGT		**Exhaust heat exchanger**	
Ambient pressure	101.3 kPa		
Turbine outlet temperature	593 ° C	Effectiveness	0.80
Compressor & turbine efficiency	0.76	Cold water inlet temperature	80 ° C
Combustion efficiency	0.99	Cold water mass flow rate	1.616 kg/s
Recuperator efficiency	0.74	Correction factor of mean temperature difference	0.965
Mechanical efficiency	0.97	Capacity ratio	0.054 ~ 0.063
Rated revolution speed	96,300 rpm	**Absorption heat exchanger**	
Rated electrical power output	28 ± 2 kW		
Electrical efficiency	26 ± 2 %	Cooling outlet temperature	7 ° C
Pressure ratio	3.4	Heating outlet temperature	55 ° C
NOx emission	<9ppmV@ 15 %O_2	Standard cooling capacity	25 kW
Rated speed of biogas compressor	450 ~1200rpm	Standard heating capacity	35.7 kW
Biogas inlet outlet pressure	0.02~6bar	Standard heat rejection to cooling tower	60.7 kW
Flow rate	~ 30Nm^3/h	Standard heat medium input capacity	35.7 kW

Table 2. Temperature range and duration of sampling day for all temperature conditions used for the analysis.

No.	Name of period (–)	Sampling days (day)	Temperature range (°C)
1	Summer	133	12 ~ 22
2	Winter	192	-3 ~ 5
3	Summer peak	20	20 ~ 30
4	Winter peak	20	-15 ~ -5
5	Annual average	365	4 ~12

Figure(s)

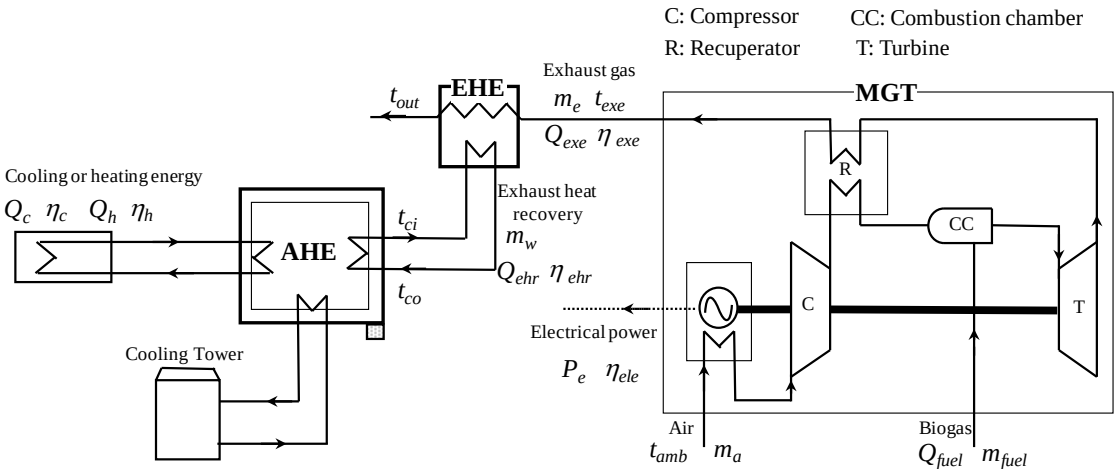

Fig. 1. Schematic diagram of the MGT-CGS.

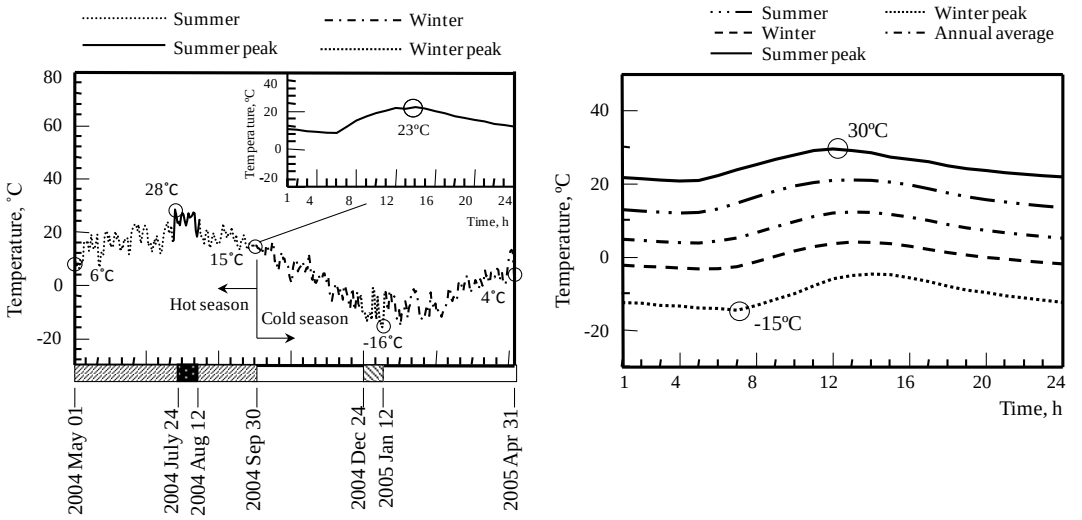

(a) Daily average temperature

(b) Hourly average temperature for all setup temperature condition

Fig. 2. Daily and hourly average temperature changes in the analysis period.

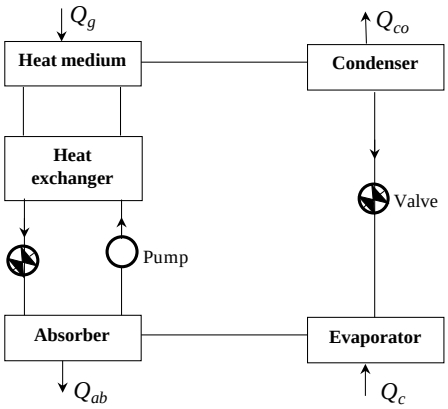

Fig. 3. Block diagram of the absorption heat exchanger (AHE).

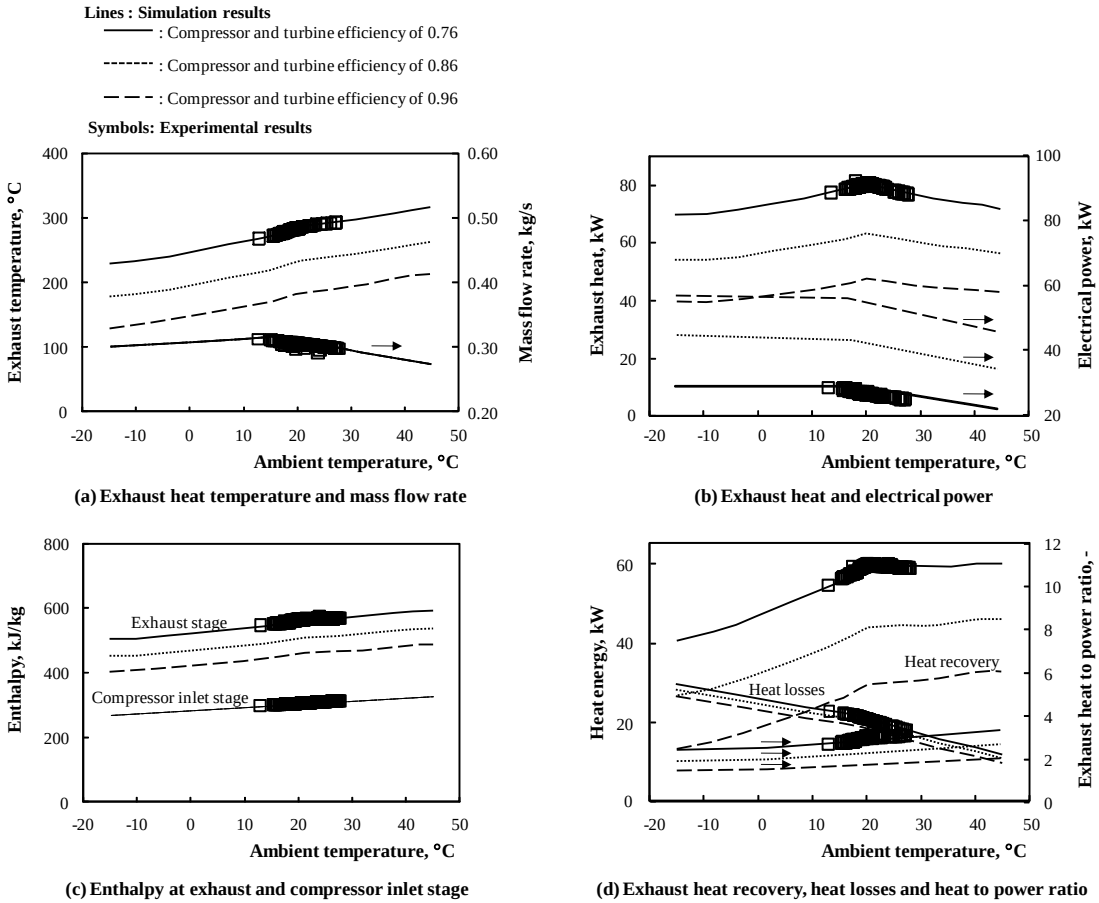

Fig. 4. Comparison of analytical and experimental results of the CGS.

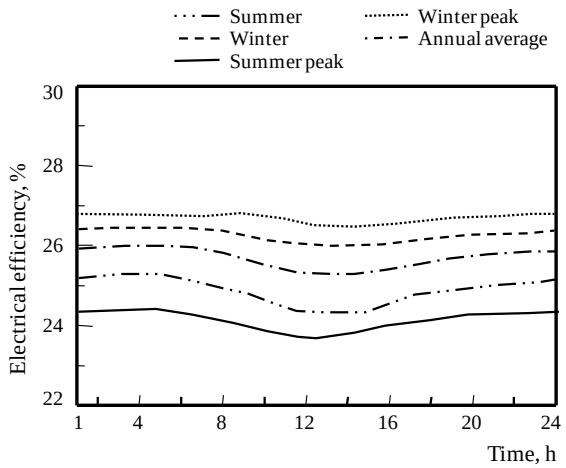

Fig. 5. Variations of electrical efficiency in all temperature conditions.

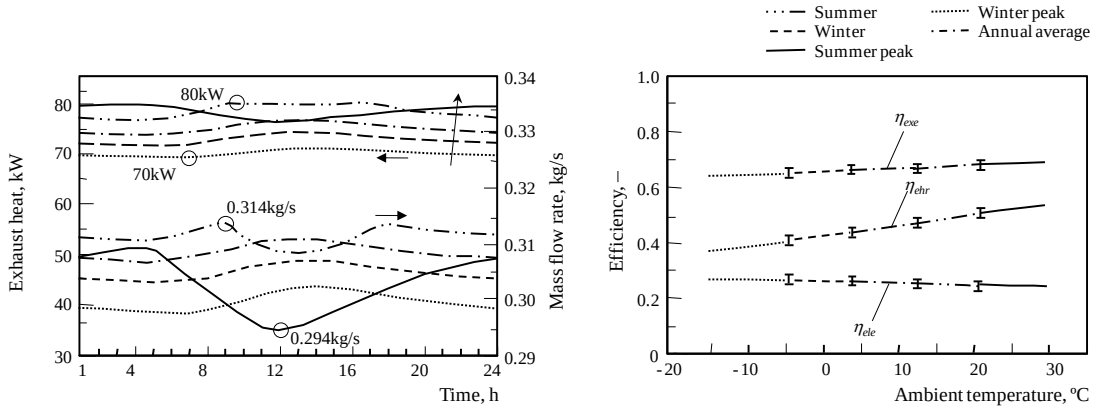

(a) Exhaust temperature and mass flow rate (b) Efficiency

Fig. 6. Mass flow rate and exhaust heat conditions, and relation of ambient temperature with efficiencies of the MGT-CGS in all temperature conditions.

Figure(s)

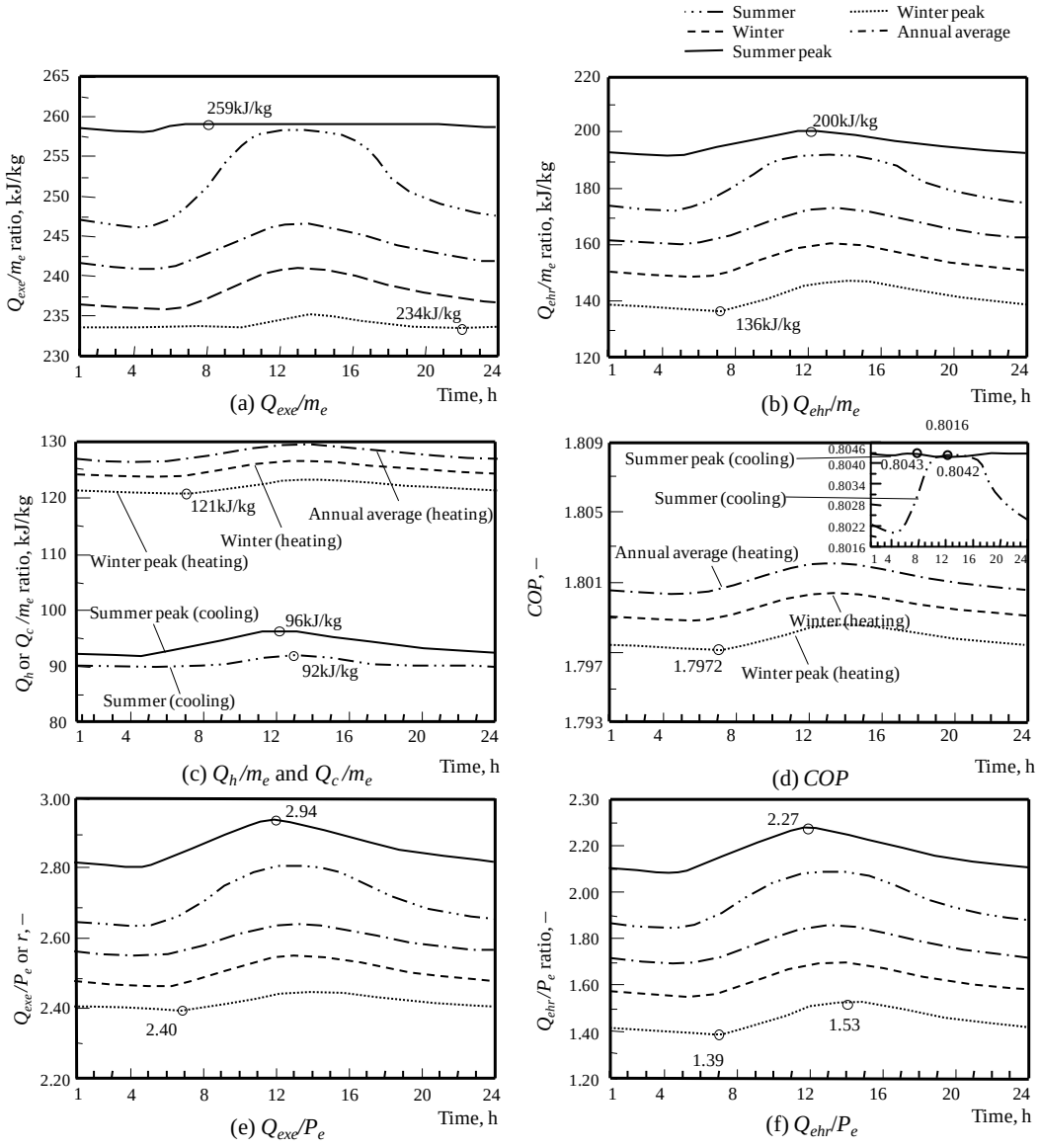

Fig. 7. Variations of heat to mass flow rate, heat to power ratio and *COP* value of the MGT-CGS for all setup temperature conditions.

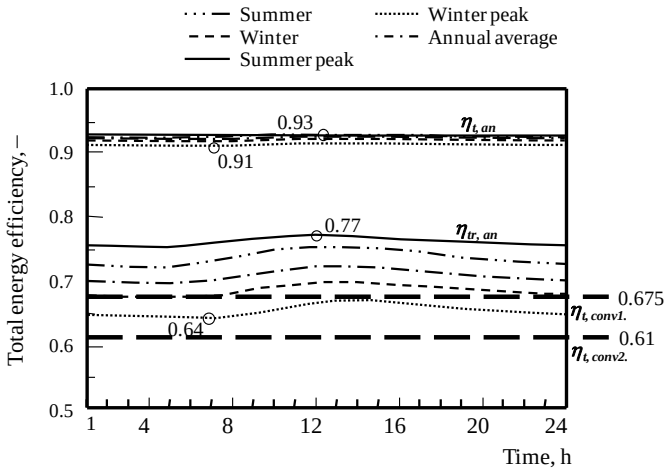

Fig. 8. Total annual energy efficiency of the MGT-CGS and conventional system for all temperature conditions.

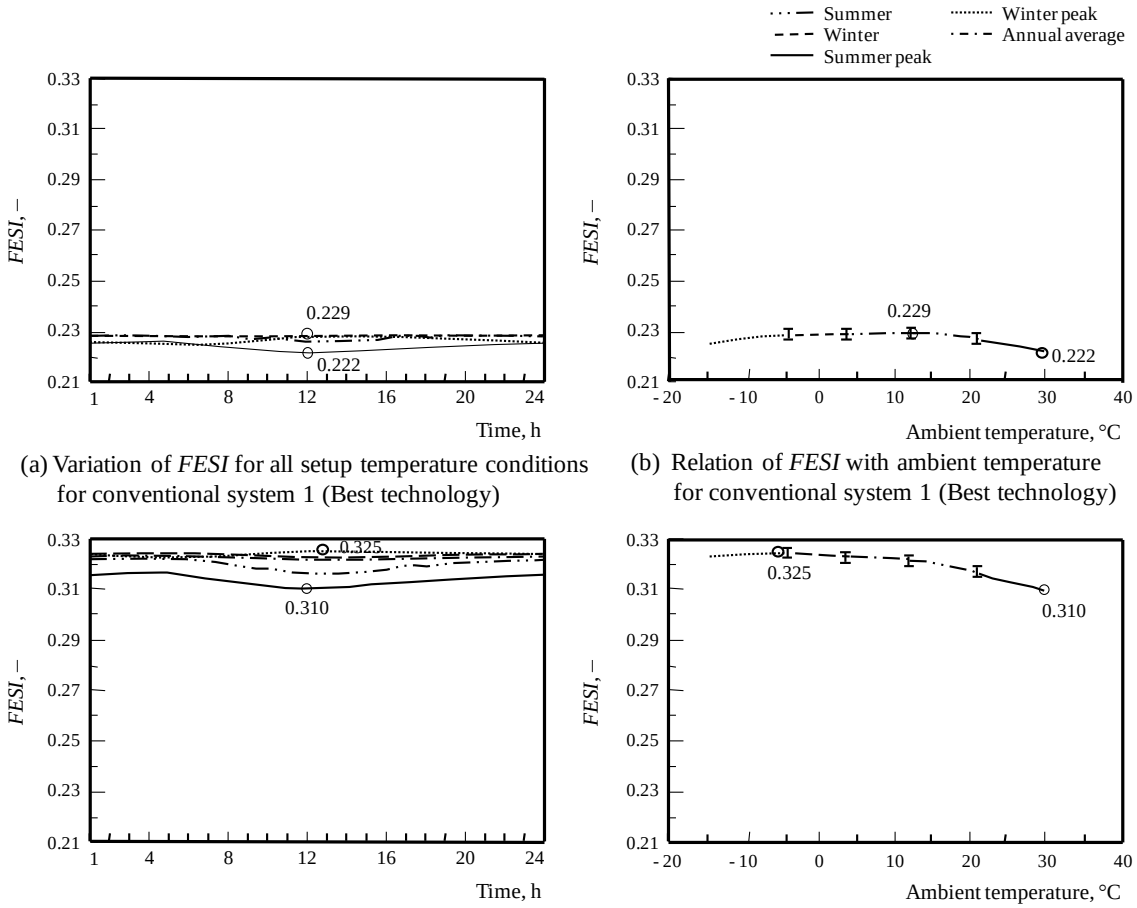

(a) Variation of *FESI* for all setup temperature conditions for conventional system 1 (Best technology)

(b) Relation of *FESI* with ambient temperature for conventional system 1 (Best technology)

(c) Variation of *FESI* for all setup temperature conditions for conventional system 2 (Typical technology)

(d) Relation of *FESI* with ambient temperature for conventional system 2 (Typical technology)

Fig. 9. Variations of *FESI* for all temperature conditions and its relation with ambient temperature.

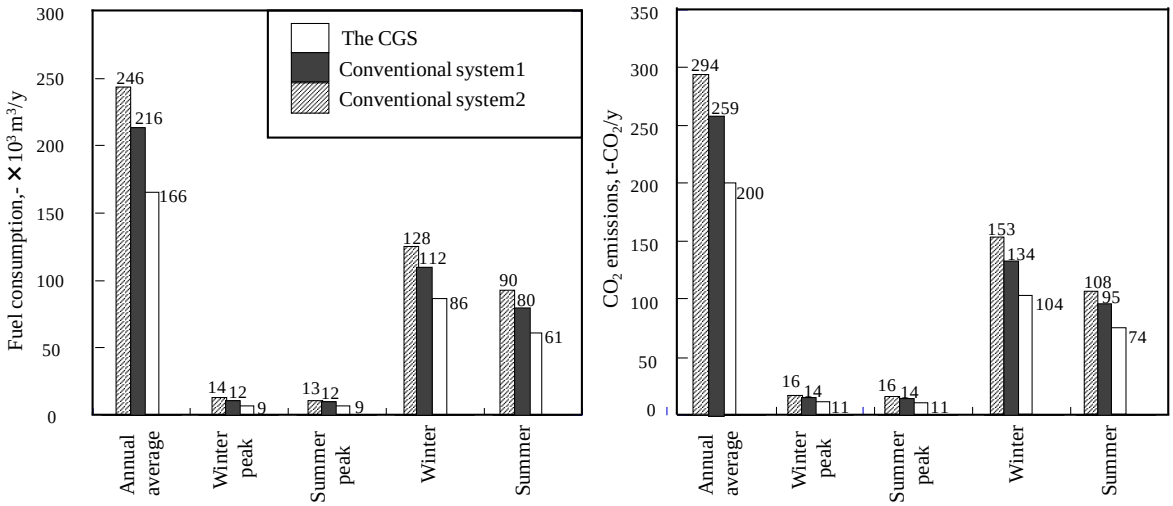

(a) Fuel consumption (b) CO_2 emissions

Fig. 10. Amount of fuel consumption and CO_2 emissions of the MGT-CGS and the conventional systems.